The Potential of Mixed Dyes of *Morus nigra L.* and *Sargassum binderi* As Photo-Absorber Layer in Solar Cell Devices

MUHAMMAD FAHMI AIZAT BIN ELIAS

F15A0282

A thesis submitted of fulfilment of requirements for the degree of Bachelor of Applied Science (Bioindustrial Technology) with Honours

Faculty of Bioengineering and Technology

Universiti Malaysia Kelantan

2019

DECLARATION

I hereby declare that the work embodied in this report is the result of the original research and has not been submitted for a higher degree to any universities of instituitions.

Student

Name : MUHAMMAD FAHMI AIZAT BIN ELIAS

Matric Number:

Date :

Approved by :

Supervisor

Name : DR. HASYIYA KARIMAH BT. ADLI

Cop :

Date :

ACKNOWLEDGEMENT

In the name of Allah the most merciful, thank you for blessing and giving me strength and ability to complete this final year project. I would like to acknowledge my deepest gratitude to my great supervisor, Dr Hasyiya Karimah for her supervision, guidance, constant attention, valuelable suggestion and personal support during this research and throughout the course of my study.

Besides that, my sincere thanks to all the laboratory assitants for helping and giving me co-operation in preparing the apparatus, chemicals that needed for this experiment. They also allowing me to access the laboratory and guidance me when I needed it.

Finally, my best regard to my course mates especially my teammates under the same supervision who always helped me and shared the information with me during my research. My deepest thank and gratitude also goes to my family for their support either mentally and financially. By and large, this report was the output of the hardwork and cooperation from all parties besides my effort.

TABLE OF CONTENTS

LIST OF TABLES

LIST OF FIGURES

LIST OF ABBREVIATION AND SYMBOLS

%	Percentage
4PP	Four Point Probe
CdTe	Cadmium Telluride
CIGS	Cooper Indium Gallium Selenide
DSSC	Dye-Sensitized Solar Cell
Eg	Bandgap Value
EIS	Electrochemical Impendence Spectroscopy
HOMO	Highest Occupied Molecular Orbital
I_2	Iodine Crystal
ITO	Indium Tin Oxide
IV	Current Voltage
LUMO	Lowest Unoccupied Molecular Orbital
M	Mulberry
m	Metre
nm	Wavelength
^{o}C	Degree Celcius
PCE	Power Conversion Efficiency
PSC	Polymer Solar Cell
S	Seaweed
SEM	Scanning Electron Microscopy
Si	Silicon
TGA	Thermogravimetry Analyzer
TiO_2	Titanium (IV) Dioxide

UV-vis	Ultraviolet Spectroscopy
V	Voltage
XM:YS	(X,Y= number)
Ω	Ohm

The Potential of Mixed Dyes of *Morus nigra L.* and *Sargassum binderi* As Photo-Absorber Layer in Solar Cell Devices

ABSTRACT

The application of natural plant-derived dyes as photo-absorber in solar cells application, have been extensively studied and proven. Natural plant-derived dyes are known containing natural compounds (e.g. carotenoids, chlorophyll, anthocyanin) that have the characteristics of electronic delocalization in extended π-orbital system involving in electronic transfer mechanism. Hence, the mixture of *Morus nigra L.* (mulberry, **M**) and *Sargassum binderi* (seaweed, **S**) were successfully prepared and several physical characterizations were carried out such as UV-vis, TGA and SEM to analyse the photo-absorber (sensitizer) properties. From the results obtained, by adjusting the ratios of **M**:**S** into 1:10, 3:1, 30:1, the wavelength of photo-absorbers were slightly changed. TGA result showed that **S** has higher melting point than **M**. Meanwhile for SEM results, the **M** dye particles on titanium dioxide (TiO_2) were in porous structure with smooth surface and the existence of both distinct shapes of both individual dye (**M** and **S**). The highest conductivity was recorded by 30**M**:1**S** with the value 0.629 V followed by the 3**M**:1**S** with the value of 0.563 at the distance of 15 cm from source of light . The result pattern was found similar trend to the previous analysis by four point probe, which mixed dyes can conduct more electricity compare to single dye. From the results, it show that mixed dye performed higher solar efficiency compared to the individual dye (**M** and **S**), as example, the mixed ratio of 30 **M**:1 **S** formed $9.44\text{x}10^{-02}$ % of solar efficiency with **M** and **S** only $9.2\text{x}10^{-02}$ % and $3.68\text{x}10^{-02}$ % respectively. Overall results suggesting that by adjusting the ratio mixture of mixed dyes solution, the photo-absorber properties and the solar efficiency values were differed and with slight modification method, better electrical conductivity can be expected for solar cells application.

Keywords: conductivity, solar efficiency, natural dyes extracts, mixed dye, co-sensitizer.

Potensi Campuran Pewarna Daripada *Morus nigra L.* dan *Sargassum binderi*

Sebagai Lapisan Penyerap Cahaya Dalam Peranti Solar Sel

ABSTRAK

Penggunaan pewarna tumbuhan semulajadi sebagai penyerap cahaya dalam aplikasi sel suria, telah banyak dikaji dan dibuktikan. Pewarna berasal dari tumbuh-tumbuhan semulajadi diketahui mengandungi sebatian semulajadi (seperti karotenoid, klorofil, anthocyanin) yang mempunyai ciri-ciri pentaksempatan elektronik dalam sistem pemanjangan orbital-π yang terlibat dalam mekanisme pemindahan elektronik. Oleh itu, campuran *Morus nigra L*. (mulberry, **M**) dan *Sargassum binderi* (rumpai laut, **S**) telah berjaya disediakan dan beberapa ciri fizikal telah dijalankan seperti UV-vis, TGA dan SEM untuk menganalisis cahaya penyerap (pemeka). Dari hasil yang diperoleh, dengan menyesuaikan nisbah **M**:**S** ke 1:10, 3: 1, 30: 1, terdapat sedikit perubahan penyerap cahaya pada luang jalur. Keputusan TGA menunjukkan bahawa S mempunyai takat lebur yang lebih tinggi daripada **M**. Sementara itu untuk keputusan SEM, zarah pewarna **M** pada titanium dioksida (TiO_2) berada dalam struktur berliang dengan permukaan halus dan wujudnya bentuk yang berbeza dari kedua-dua pewarna individu (**M** dan **S**). Kekonduksian tertinggi direkodkan dengan 30**M**:1**S** dengan nilai 0.629 V diikuti dengan 3**M**:1**S** dengan nilai 0.563 pada jarak 15 cm dari sumber cahaya. Corak yang terhasil didapati menyerupai dengan trend analisis sebelumnya dengan empat titik penyelidikan, yang pewarna bercampur boleh melakukan lebih banyak elektrik dibandingkan dengan pewarna tunggal. Dari hasilnya, menunjukkan bahawa pewarna bercampur menghasilkan kecekapan sola yang lebih tinggi berbanding pewarna individu (**M** dan **S**), contohnya, nisbah campuran 30**M**:1**S** membentuk 9.44x10-02% kecekapan solar dengan **M** dan **S** sahaja 9.2x10-02% dan 3.68x10-02%. Keseluruhan data menunjukkan bahawa dengan penyesuaian nisbah campuran pewarna campuran, ciri-ciri penyerap-cahaya dan nilai-nilai kecekapan sel suria berbeza dan dengan sedikit pengubahsuaian kaedah, kekonduksian elektrik yang lebih baik boleh dijangka untuk aplikasi sel suria.

Kata kunci: kekonduksian, luang jalur, elektronik, campuran, ekstrak pewarna semulajadi, pemeka.

CHAPTER 1

INTRODUCTION

1.1 Background of Study

Energy crisis

Many people believe that energy problem is amongst the biggest challenges for human kind in the 21st century. The demand is due to the increasing of world population in which some studies predict world population will be increased up to 9 billion in 2040, from 7 billion people today (Guarracino *et al.*, 2017). Thus, the increasing of living things, mostly humans will eventually lead to an increase of energy demand.

The solar energy can be converted into electricity, directly using devices based on semiconductor materials, which is also known as photovoltaic. Following the exploration, the dye-sensitized solar cell (DSSC) has been introduced to imitate photosynthesis mechanism. Initially, ruthenium (Ru) material has been used as photosensitizer, due to its high stability in oxidized state and its properties which is positivity electrochemical. However, the usage of Ru material is not favourable due to toxicity issues and high cost (Ayalew & Ayele, 2016). The porphyrin dyes invented later by Simon Mathew performed high power conversion efficiency (PCE). However, these materials were complex to produce and had carcinogenic nature and non-biodegradability (Sawhney & Satapathi, 2017). Following that exploration, natural dyes becomes the other choice to replace traditional synthetic dyes considering its ease of preparation, cheaper, eco-friendly, non-toxic and biodegradable (Gong et al., 2017). Natural dye can be extracted from various fruits, leaves, and vegetables that has various colour.

In this study, natural dyes of *Morus nigra L. sp.* (Mulberries) & *Sargassum binderi sp.* (seaweed) were extracted and the mixed dye from these two extract dye had been prepared. The electrical conductivity and characterizations such as, Scanning Electron Microscopy (SEM), Ultraviolet-visible Spectrometer (UV-Vis), Four point probe (4PP) and digital multimeter had been done to explore the ability of these prepared natural dyes for solar cell application.

1.2 Problem Statement

Humans nationwide still depend on fossil fuel although the source of energy is scarce, almost depleted and its production causes a lot diverse effect to the environment. Recently, a lot of studies had been carried out to explore new energy source to replace fossil fuel. One of the solutions is by converting solar energy into electricity, or also known as solar energy technology. But this technology is still new and considered premature, thus it needs in-depth investigation in order to challenge the traditional energy.

Due to the high cost of manufacturing and environmental impact originated from polycrystalline, poly-amorphous and mono-crystalline of the semiconductor materials of solar cells, other material candidates of solar cells were introduced such as dye-sensitized solar cells (DSSCs). DSSC had emerged as low-cost solar cell with comparable solar efficiency and superior advantage of easy to fabricate. Furthermore, natural dyes used for DSSC are easier to be extracted from plentiful plants, even from agricultural wastes. Therefore, DSSC should be considered as a prospect energy source that could be endured and sustained. From previous study, there are several kind of DSSC that only focusing on individual dye and the solar cell efficiency is low. The study of mixed dye is expected to give more absorbance of light and conduct better electricity due to changes in its physiochemical properties.

1.3 Objectives

The objectives of this study are as the following:

1. To produce homogenous mixture solutions of extract dye in the ratios of (**M**:**S**; 3:1, 1:10 and 30:1) from extracted dyes of *Morus nigra L.* (mulberries) (**M**) *Sargassum binderi*. (seaweed) (**S**) and as potential photosensitizers in solar cells.
2. To carry out the series of physical analysis using instruments such as Ultraviolet-Visible Spectroscopy (UV-Vis), Scanning Electron Microscopy (SEM), Four Point Probe (4PP), Thermogravimetric analyzer (TGA), Differential Scanning Calorimetry (DSC) and Electrochemical Impedance Spectroscopy (EIS).

3. To evaluate and compare the conductivity and solar cell performance of single and mixture dyes using digital multimeter and four point probe.

1.4 Scope of Study

Overall stage in this study is summarized below.

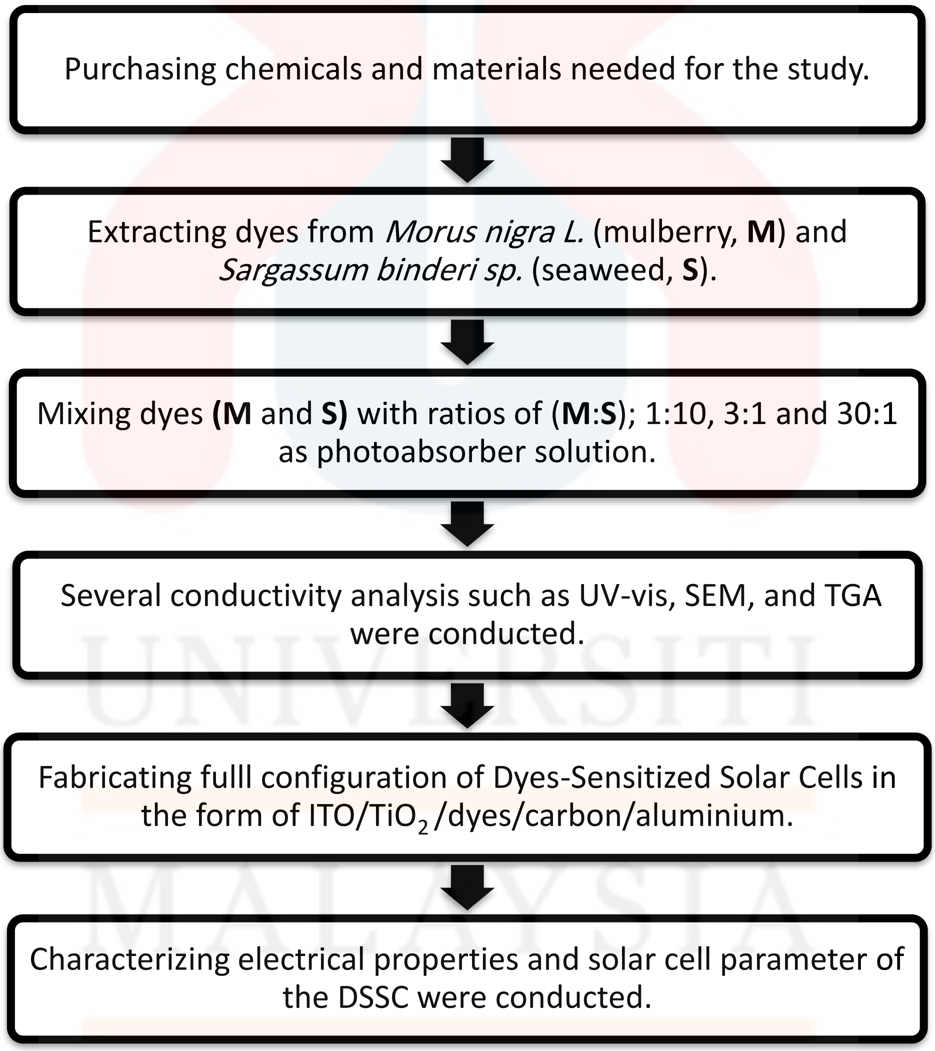

Figure 1.0 : The work flow method.

1.5 Significance of Study

This study is significant as the knowledge in dye-sensitized solar cell (DSSC) and the application of suitable natural dyes extracted from plants and fruits sources in Malaysia as efficient photoactive layer in can be developed in bigger spectrum. On top of that, the result of electrical conductivity in DSSC with *Morus nigra L. sp.* (Mulberries) and *Sargassum binderi sp.* (Seaweed) will hint their potential in DSSC, and hopefully it will narrow down the existing gaps between theoretical and practical aspects of DSSC based on natural extracted dyes, specifically based on the optimized hybrid dyes solution.

CHAPTER 2

LITERATURE REVIEW

2.1 Global Energy Issue

As humans, we are depending on energy to do our daily routines. Energy used by different users can be divided into five class, which are residential, commercial, industrial, electric and transportation (Kao Circle, Manassas C, 2017). Residential building are any place that people live, while commercial building includes offices, stores, hospital, restaurants and school. This two sectors use energy for heating during cold season and cooling during summer time. These two residential and commercial buildings also use energy for lighting and nowadays, mostly commercial building use fluorescent lighting, though it costs more money for installation purpose but it uses less energy to produce the same amount of light (World Energy Council, 2013). Whereas, industrial sector consumes more energy, for example petroleum refining, aluminium manufacturing and steel manufacturing. Energy used in transportation such as automobile, commercial transportation, trucks, trailers, airplane and mass transit are very massive. However, the biggest amount of usage of electric according to Jager et al., (2014) is the electric, while commercial and residential uses only 4.2% and 6.5%, respectively. Figure 2.1 below show the percentage of the usage of energy in 2015 (Jager *et al.*, 2014)**.**

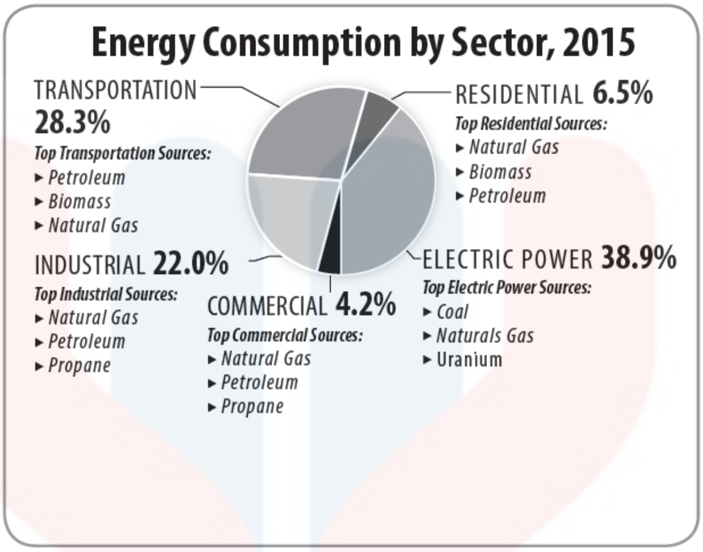

Figure 2.1 : Energy consumption by sector (Jager *et al.*, 2014)**.**

Energy consumed for electric power is the biggest portion whereas the second large energy consumption is for transportation, followed by industrial use. Fuel is the biggest operating cost for all vehicles therefore, making these automobile more energy-efficient is very important. The increasing demand in energy has economic impact, as well. If there is more demand for energy, while energy supply does not change much, the product will be more expensive. Among the challenges that our energy infrastructure depends heavily on fossil fuels like oil, coal and gas. The problem is that humans deplete these fossil fuels deplete much faster than they are generated, therefore fossil fuels are not a sustainable energy source (Jager *et al.*, 2014).

In terms of the environmental impact, solar power is a better and more optimal resource than fossil fuels. Although for reliable application, fossil fuels offer various benefits of being a reliable resource that offer near-constant availability. The detriments of gas, oil and coal cause significant pollution and its scarce resource will eventually run out (Luke Richardson, 2017). On the other hand, solar energy is easily installed on a rooftop surface or ground mount but in comparison, fossil fuel requires the degradation of the earth as means for fuel production. The production of fossil fuels just not merely creates greenhouse gas emissions, it also degrades and erodes the ground and pollutes water supply (Jager *et al.*, 2014).

Figure 2.2 shows the distributions of traditional energy (fossil fuel) and various type of clean energy (e.g, hydropower, nuclear, solar, wind, biomass and geothermal). It is clearly shown that the percentage of clean energy is expected to increase in another few decades, in which might overcome the dependence on fossil fuel resource (Deep Resource, 2015).

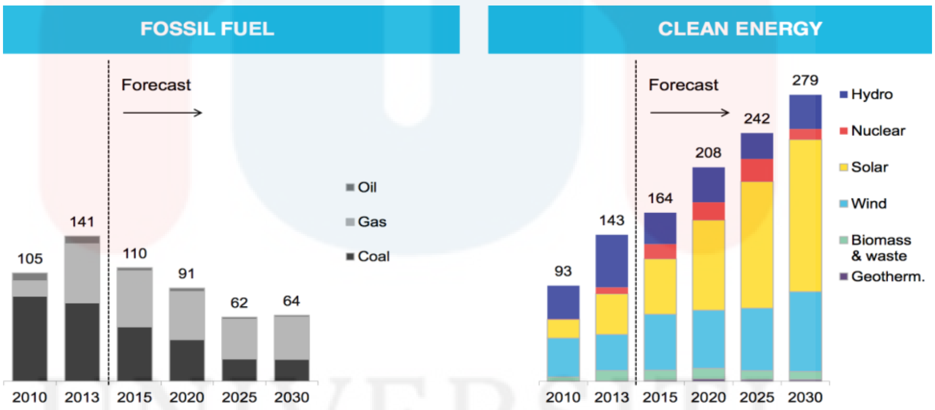

Figure 2.2: The future of energy usage in electric generating capacity (Deep Resource, 2015).

2.2 Solar Energy and Electricity

It is predicted that up to 2030 the world's required total energy will be doubled due to world's population growth and economic growth. Also, fossil fuels price and impact on the environment, namely green-house effect, is an important issue. Then, there is a growing need for clean and reproducible energy sources. Solar energy is known as one of the main source of clean energy (Abbasian *et al.*, 2012). The development of solar energy on a commercial basis turned out to be a lengthy process whose progress was primarily shaped by the price and cost of alternative conventional energy sources. Solar was especially vulnerable to the price of competitor sources of energy as it emerged as the most expensive renewable energy. Innovation was driven by visionary entrepreneurs, all of whom faced the problem that solar industry is a highly capital-intensive and technologically-complex product. This led them to seek investments from large established firms in industries, especially electronics and petroleum, and to rely on public policy to facilitate the growth of the industry (Jones and Bouamane, 2012).

The sun is responsible for all of the earth energy. Plants use the sunlight to make food. Decaying plants hundreds of millions of years ago produced the coal, oil and natural gas that we use today. Solar energy is collected by using solar cells. Solar energy can be put to use to heat or light up a room by simply having well placed windows and skylights. People can also use solar energy to dry our clothes in the sun. Solar cells are used to collect solar energy to power up electrical appliances. With the depletion of energy source in the world, solar energy source will play an important role in the development. So the renewable solar energy source is the best choice (Jingcheng, 2010). Also, fossils fuels are facing rapid resource depletion, but the demand for energy is growing day by day and many countries around the world have no alternative but to increase domestic oil process. So there is an urgent need of sustainable energy resources, such as the solar energy, which is considered as an environmentally friend, novel alternative and promising candidate to address this problem. However, solar energy has a limited application that directly related to its high cost of the per watt electricity generated. It is important to transform these solar energy into electric energy (Al-Bat'hi, Alaei and Sopyan, 2013).

Reportedly, it is estimated that sunlight can radiate more energy in daily (1.34x1031 J/day) which can satisfy the world's energy requirements in a whole year (Moser, 2005). Only a slight part of the visible radiant energy (light) emits by the Sun into the space ever reaches the Earth horizon, but there is still additional light as to source the prevalent energy needs (Kao Circle & Manassas, 2017). Solar cells and photo detectors are devices that can convert an optical input into current. A solar cell is an example of a photovoltaic device, which is a device that generates voltage when exposed to moving around in semiconductor cause an electric current formed (Bhatia, 2014). The photovoltaic effect was discovered by Alexander-Edmond Becquerel in 1839, in a junction formed between an electrode and an electrolyte.

2.3 Solar Cell Generation

The idea of using the power of the sun for heating and lighting purpose was intuitive. Since early mankind, passive solar energy has served as a form of light and heat to human. In the 5th century B.C., the ancient Greeks homes' lay out are designed to be able capture the sun's heat during winter seasons. Later, the improvisation on solar architecture is made by the Romans, by covering south-facing windows with clear materials such as mica or glass, to prevent the solar heat captured during the daylight from escaping. In the 1760s, the Swiss scientist Horace de Saussure has invented an insulated rectangular box with a glass cover that later has became the prototype for solar collectors which function is to heat water (Jones and Bouamane, 2012).

The fabrication of solar cells has passed through a large number of improvement steps from one generation to another. Silicon based solar cells were the first generation solar cells grown on Si wafers, mainly single crystals (Sharma *et al.*, 2015). Further development to thin films, dye sensitized solar cells and organic solar cells had enhanced the cell efficiency. The development is basically hindered by the cost and efficiency (Sharma, Jain and Sharma, 2015). A solar cell is a photovoltaic device that generates voltage when exposed to light. The penetration depends on the wavelength and the absorption coefficient increases as the wavelength decreases. Power sources based on photovoltaic is required for back-up from energy resources or as energy storage during the night (Al-Bat'hi, Alaei and Sopyan, 2013).

As mentioned earlier, the solar cells are originated from the production on silicon wafers. The efficiency of its high power has made it the oldest and the most popular technology. The silicon wafer based technology is later classified into two subgroups, which are 1) single/ mono-crystalline silicon solar cell and 2) poly/multi-crystalline silicon solar cell. This generation solar cell which conventionally doped with another element to give their negative or positive charge based on their electronic charge carriers. During the manufacturing process, Si crystals are sliced from the big sized ingots. These large single crystal productions require precise processing because the recrystallizing process of the cell requires more costs and will need to undergo various process. The efficiency of mono-crystalline single-crystalline silicon solar cells is between 17% to 18% (Bertolli, 2008). The processing of polycrystalline Si solar cells is viewed as more economical, for they are produced by cooling a graphite-mould filled which contains molten silicon and are currently regarded as the most famous solar cells.

This solar cell has been dominated commercials since few decades ago because of high efficiency despite its high manufacture costing. In 2008, they are believed to occupy up to 48% of the solar cell production worldwide (Čekon and Rovnaník, 2015).

Most of the thin film solar cells and amorphous silicon (a-Si) solar cell are second generation solar cells, and they are more economical as compared to the first generation silicon wafer solar cells. Silicon-wafer solar cells are built of light absorbing layers which is equal to 350 µm thick, whereas thin-film solar cells are composed of very thin light absorbing layers, generally of the order of 1 µm thickness (Chopra *et al.*, 2004). Second generation of solar cell having stacks of films (photo-absorber) that absorb light in different wavelength. This solar cell requires less material for its design compare to first generation, which then could lower the manufacturing cost. The best materials that have reported previously were amorphous silicon (Si), cooper indium gallium selenide (CIGS) and cadmium telluride (CdTe), in which some elements that are utilized are toxic and unstable (Sharma *et al*., 2015).

Third generation cells are the new promising technologies but are not commercially investigated in detail. Most of the developed third generation solar cell types are nano-crystal based solar cells, polymer based solar cells, perovskite solar cells and dye sensitized solar cells. While for third generation solar cell technology, it has high potential to become advanced solar cells. All these solar cell are the most promising solar cells (Gong *et al*., 2017). These solar cells are known able to overcome the lower efficiency of second generation with lower manufacturing cost. Nano-crystal based solar cells are generally also known as quantum dots solar cells. These solar cells are composed of a semiconductor, generally from transition metal groups which are in the size of nano-crystal range made of semiconducting materials. Quantum dots is just a name of the crystal size ranging typically within a few nanometres in size, for example, materials like porous silicon (Si) or porous TiO_2, which are frequently used in quantum dots (Bertolli, 2008). In line with the advancement of nanotechnology nowadays, nano-crystals of semi-conducting materials are aimed to be the replacement of semiconducting material in bulk states such as silicon (Si), cadmium telluride (CdTe) or cooper indium gallium selenide (CIGS) (Collins *et al*., 2000). Polymer solar cells (PSC) are generally flexible solar cells due to the polymer substrate. The first PSC were invented by the research group of Tang *et al* in year 2016 (Herman *et al.*, 2011). A polymer solar cells is composed of a series of connected thin functional layers coated on polymer foil or ribbon. The function is usually as combination of donor (polymer) and an acceptor (fullerene). In fact, there are various types of materials for the absorption of sunlight, as well as organic material which can act as connector / conducting polymer (Ginger and Greenham, 1999). The first dye-sensitized solar cell (DSSC) was introduced by Michel Grätzel in Swiss Federal Institute of Technology (O'Regan and Grätzel, 1991). DSSC generally employs dye molecules between the different electrodes.

2.4 Dye-Sensitized Solar Cell (DSSC)

Since their invention in 1991, dye-sensitized solar cells (DSSCSs) have been extensively studied as an alternative kind of solar cells, owing to their simple structure, transparency, flexibility, low production cost and wide range of application (Yang *et al.*, 2014). Despite these advantages, the low efficiency of DSSC still cannot compete with that of silicon-based cells, which limit their commercial implementation. Consequently, there is a critical need to improve the solar efficiency of state-of-the-art DSSC in order to realize next generation solar cells. In comparison with high-cost conventional silicon solar cells, dye-sensitized solar cells are well known as a cost-effective photovoltaic device because of inexpensive materials and simple fabrication process (Rehm *et al.*, 1996). DSSC are composed of titanium oxide (TiO_2) semiconductor and the dye sensitizer that can be extracted from a variety of natural resources with minimum costs. As such, DSSC are easy to fabricate since they are insensitive to environment contaminants and processable at variant temperature (Guarracino *et al.*, 2017).

DSSC are composed of four parts. The first part is the electrode film layer of titanium dioxide (TiO_2), covered by a monolayer of dye molecules that absorbs solar light (Al-Bat'hi, Alaei and Sopyan, 2013). TiO_2 layer facilitates charge transfer from the dyes to the electrode layer. The third component is the counter electrode layer (e.g carbon) and the presence of the redox electrolyte layer to reduce the level of energy supplied from the dye molecules (Sumardiasih *et al.*, 2017).

In DSSC, sensitizing dyes plays a key role in absorption of light and the transformation of solar energy into electrical energy. Although DSSC have provided high relative efficiency, use of precious metals like ruthenium (Ru) complexes is its disadvantages which are noble metals considered as limited resources, so its production requires a very large cost. Moreover, the organic dyes are not only cheaper but have been reported to show efficiency of 9.8 %. (Cerda *et al.*, 2016). Natural dyes found in flowers, leaves and fruits can be extracted by simple procedure. Due to its cost efficiency and non-toxicity, natural dyes have been a popular research topic. Until now, various natural dyes have been used as sensitizers in DSSC, such as carotene, anthocyanin and chlorophyll. DSSC composed of a porous layer of titanium dioxide nanoparticles, covered with a molecular dye that absorbs sunlight. Charge separation occurs at the surfaces between the dye, semiconductor and electrolyte (Swami, 2012). Figure 2.3 above show the charge separation occur in DSSC (Ranabhat *et al.*, 2016).

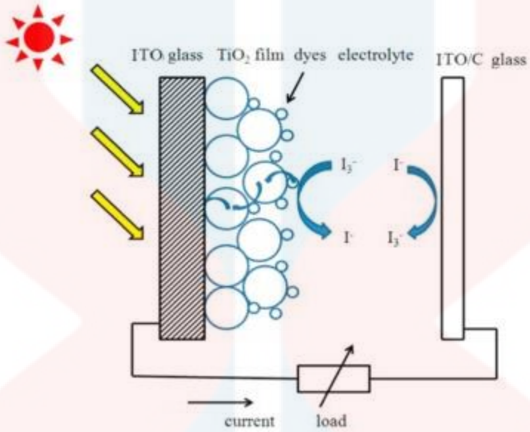

Figure 2.3: The mechanism in DSSC (Ranabhat *et al.*, 2016).

2.5 Hybrid Approach of Natural Dye Extract

Dyes derived from natural materials such as plant leaves, roots, bark, insect secretions and minerals are the dyes that widely use for the colouring of textiles until the discovery of the first synthetic dye in 1856 (İnanç, 2011). Vigorous research in the synthetic chemistry along with the industrialization of textile manufacturing has led to the development of synthetic dyes, and also acceleration in the number of synthetic dyes in assorted hues and colours which has then gradually shifted natural dyes into oblivion. Starting from the latter half of nineteenth century, the use of natural dyes started to decline after the invention of synthetic dyes. However, environmental issues arise from production and application of synthetic dyes has once again revived consumer attraction to natural dye since the last few decades (Saxena and Raja, 2015). Natural dyes are considered eco-friendly as they are renewable, sustainable and bio- degradable. Natural dyes can be applied for dyeing purpose of nearly all sorts of natural fibers. New research shows that they also be can applied to dye some synthetic fibers. Apart from their application in textiles, natural dyes can also be used in the food coloration, medicines, handicraft items and toys, in leather processing. On top of that, many of the dye-yielding also served as medical or ointment purpose in various traditional medicinal set-up. In addition, dye also can be used in DSSCs as photo-absorber (Osabohien, 2014).

The dyes from natural resources are based upon their source of origin classified as plant, animal, mineral and microbial dyes. Anthocyanins are generally accepted as the largest and most important group of water soluble pigments in nature (Jager *et al.*, 2014). They are responsible for the blue, purple, red and orange colours of many fruits and vegetables. Mulberry fruit is a well-known source of anthocyanins with many biological activities (Aramwit, Bang and Srichana, 2010). The diversity of anthocyanins are due to the numbers of hydroxyl and methoxyl groups on the basic anthocyanin skeleton and the number of sugars are attached (Wahyuono and Risanti, 2012). Mulberry fruit changes the colour from green to black purple through red with maturity. Some varieties introduced from mid Asia have white fruits. Figure 2.4 shows the basic anthocyanin structure derived from mulberry (László, 2015).

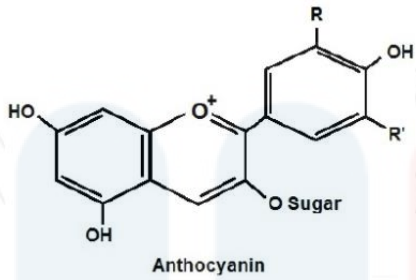

Figure 2.4: Anthocyanin structure (László, 2015).

Meanwhile, chlorophyll is the green pigment utilized by all higher plants for photosynthesis. Its name is derived from the Greek *"chloros"* that mean green and *"phyllon"* which mean leaf. Chlorophyll is a cyclic tetrapyrrole with coordinated magnesium in the centre, as shown in Figure 2.5 (Yuri Tsuruda *et al.*, 2013). Because of the lability of the coordinated magnesium and the associated colour change, chlorophyll is used as colorant (Yip *et al.*,2014).

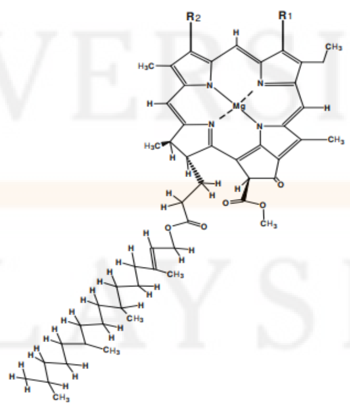

Figure 2.5: Chemical structure of chlorophyll (Yuri Tsuruda *et al.*, 2013).

CHAPTER 3

METHODOLOGY

3.1 Materials

3.1.1 Chemicals and Reagents

Titanium (IV) dioxide (TiO_2) nano powder, indium tin oxide (ALDRICH®), detergent, methanol absolute (EMSURE®), acetonitrile (Merek LiChrosolv®), ethanol absolute (HmbG® Chemicals), potassium iodide, carbon (graphite), ethylene glycol (R&M Chemicals), iodine (I_2) pearl (HmbG Chemicals) and aluminium coated glass. Natural dyes were extracted from *Morus Nigra L. Sp.* (Mulberries, **M**) collected from nearby resident *& Sargassum binderi sp.* (seaweed, **S**) collected from Kunak, Sabah.

3.1.2 Apparatus

Few apparatus also were used in this study such as magnetic stirrer, reagent bottle, hot plate, furnace, beakers, filter paper, pipette, mortar and pestle, spatula, water bath, centrifuge machine, ultrasonic bath, conductive adhesive tapes, Indium Tin Oxide

(ITO) glass, hair dryer, centrifuge tube, scotch tape, clean box, glass rod, conical flask, centrifuge tube, dropper and spatula.

3.1.3 Instruments

In completion of this study, few equipments were used to analyse the extract dyes and full solar devices, including Brunauer-Emmett-Teller (BET) (Micromeritics' ASAP® 2020) particle analyzer, Scanning Electron Microscopy (SEM) (HACH DR6000), Ultraviolet-visible Spectrometer (UV-Vis), Four Point Probe (4PP) (Jandel HM 21), Thermogravimetric analyzer (TGA), Differential Scanning Calorimetry (DSC) (Mettler Toledo GC10), Electrochemical Impedence Spectroscopy (EIS) (Metrohm Autolabs), and digital multimeter (EX540).

3.2 Methods

3.2.1 Preparation of Natural Dye

The extraction of dyes were done according to literature review with some modification (Nik Muqit, 2018). The samples of *Morus nigra L. sp.* (Mullberries) (**M**) was collected from the nearby resident in Jeli, Kelantan. The fruit samples were stored in the chiller before use. The fruit samples then were crushed using mortar and pestle and further soaked in 95% methanol and kept at room temperature overnight. After that, the samples were filtered using vacuum pump to remove excess solid residue. The filtrate was stored in dark reagent bottle and kept in the chiller.

Meanwhile, the samples of *Sargassum binderi sp.* (seaweed) (**S**) was collected from Kunak, Sabah. The seaweed was dried in oven at 100 °C for overnight before crushed into powder form and boiled. The dyes solution was prepared in 10 gram into 40 ml of 95 % methanol in a beaker for 4 hours at 60 °C. The hot solution was filtered through the filter paper to remove excess solid residue. The dye solution was stored in chiller under dark condition.

The extract dye solutions of **M** and **S** were kept under dark condition in cool temperature upon analysis and device fabrication. These solution were applied as photo-sensitizer in dye-sensitized solar cells. Figure 3.1 shows the sample before and after the extraction.

Morus nigra L. sp (mulberry) in solid form and in dye solution form.

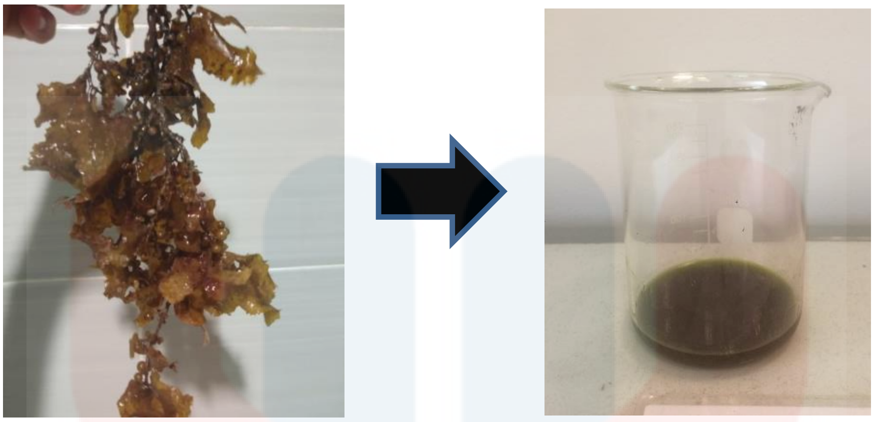

Sargassum binderi sp. (seaweed) in solid form and in dye solution form.

Figure 3.1: The dye solutions for **M** and **S.**

The mixed dyes solution containing both dyes were prepared in different ratios; 10:1, 3:1 and 30:1, denoted as X**M**: Y**S** (X, Y = number; **M** = mulberry; **S** = sargassum), e.g., when 3 mL mulberry solution was added with 1 mL seaweed is denoted as 3**M**: 1**S**. All the mixed dye were stirred using magnetic stirrer overnight to ensure homogenization. The natural dyes extracts and the mixed dye solutions were properly stored and protected from direct sunlight for further characterization.

3.2.2 Preparation of ITO glass and TiO_2 paste

ITO conductive plates are cut into 2 × 2 cm pieces. The glass were then cleaned in a detergent solution then the glass were put in an ultrasonic bath for 5 minutes. Then, the glass were washed in ethanol and put into the ultrasonic bath. Then, the glass was further rinsed with water and ethanol, and then dried with hair dryer and stored separately in different zipper bag.

While for the preparation of Titanium dioxide (TiO_2) paste, the TiO_2 nanopowder paste is prepared by dissolving 2 g of TiO_2 nanopowder into 100 ml polyethylene glycol and stirred using magnetic stirrer for 30 min until homogeneous paste is obtained. Once the homogenous paste is obtained, the paste was next diluted with 1 ml of the paste into 100 ml ethanol. Upon deposited on the ITO glass the mixture was stir overnight first to ensure the paste is homogenous.

3.2.3 Preparation of titanium (IV) dioxide (TiO_2) on Indium Tin Oxide (ITO)

First of all, the glass was dropped with one drop of ethanol to remove dust. After the ethanol was dried, 0.5 cm of the glass surface were covered with masking tape. Then, TiO_2 paste is deposited on the cleaned ITO glass surface by using the doctor blade technique. This technique were done 3 time repeatedly in 5 minutes, 10 minutes and 20 minutes drying time. After spreading the paste on ITO glass, the films were left to dry on a heater at 70 ºC for 30 minutes followed with sintering in the furnace at 500 °C for 30 minutes ramp time.

3.2.4 Preparation of electrolyte solution

Iodine crystal (I_2) was weighted into 1.08 gram then it was dissolved into the mixture solution of 20 ml of acetonitrile and 5 ml of ethylene glycol. After that, 0.35 g of I_2 crystal was added into the solution to prepare iodine mixture that later on be used as electrolyte in dye-sensitized solar cell.

3.2.5 Dye-Sensitized Solar Cell Fabrication

These TiO_2 films were then, dyed with the extracts of natural mixed dyes *Morus nigra L. sp*. (mulberries) (**M**) & *Sargassum binderi sp.* (seaweed) (**S**) by soaking the glass into respective dye solutions for overnight. After that, the resulted ITO/TiO_2 (**M** or **S**) films were left to dry on a heater at 70 ºC for 5 minutes. Three other glass also prepared using the same method but each glass were soaked into different mixed solution which is 10**M**: 1**S**, 3**M**: 1**S** and 30**M**: 1**S**. ITO/TiO_2 (10**M**: 1**S**, 3**M**: 1**S** and 30**M**: 1**S**) films were left to dry on a heater at 70 ºC for 5 minutes. The dyed TiO_2 electrode and aluminium coated glass counter electrode were then assembled with a clip to hold both glass and ready for solar cell measurement and characterization.

CHAPTER 4

RESULTS AND DISCUSSION

4.1 Introduction

This chapter discuss on the results obtained from series analysis that were carried out as stated in chapter 3. The analysis were conducted such as physical analysis observation, analysis by using Ultraviolet-Spectroscopy (UV-vis), conductivity, Scanning Electron Microscopy (SEM), thermogravimetric analysis (TGA) and differential scanning calorimetry (DSC) and 4 point probe.

4.2 Physical Observation of Extract Dyes and Mixed Dye Solution

The extract of dye and the mixed dye solution was physically observed using naked eye. As shown in the Figure 4.1, the images show the solution colour of dye extract from *Morus Nigra L* (mulberry, **M**) and *Sargassum Binderi sp*. (seaweed, **S**) and three mixed dye solutions in the ratio of 1 **M**:10 **S**, 3 **M**:1 **S** and 30 **M** : 1 **S**. All mixed dye solution were in homogenous with the new colour after mixing of both individual extract dye.

From the physical observation, it shows that the higher ratio of dye extract, (**S**) form the solution with more greener colour. When the solution is combined with more ratio (**M**), the obtained solution colour turned slightly purplish. This is the first point to highlight the mixing of both dye were successfully done.

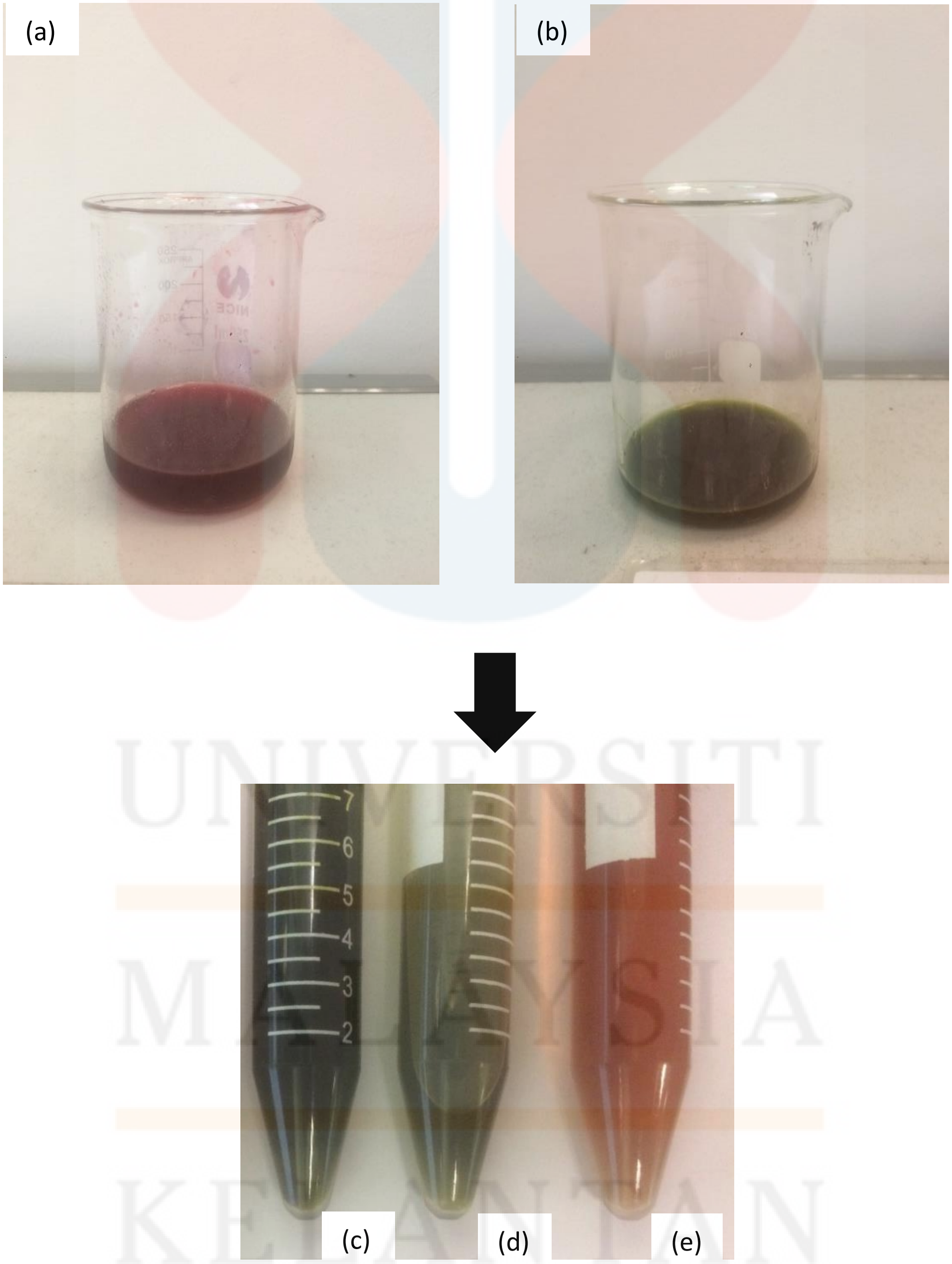

Figure 4.1: (a) **M,** (b) **S,** (c) 1**M:** 10**S**, (d) 3**M**: 1**S** and (e) 30**M**: 1**S**

4.3 Uv-Vis Absorption Analysis

The visible and ultra violet spectra of ions and molecules are only associated only with the transition between electronic energy level of the functional group of the molecules. The ultraviolet range extend from 10 - 200 nm is known as far ultraviolet while 200 - 380 nm is known as far ultraviolet. Range extend from 380-780 nm are the region for visible (Baxter *et al.*, 2008)

In this experiment, the solution of dye extracts and the mixture dyes was tested using ultraviolet-visible spectroscopy (UV-vis) (HACH DR 6000). As shown in the figure the absorption spectra of the dye extract and the mixed dye solution present in distinct absoption peak in the visible region from 400 - 800 nm.

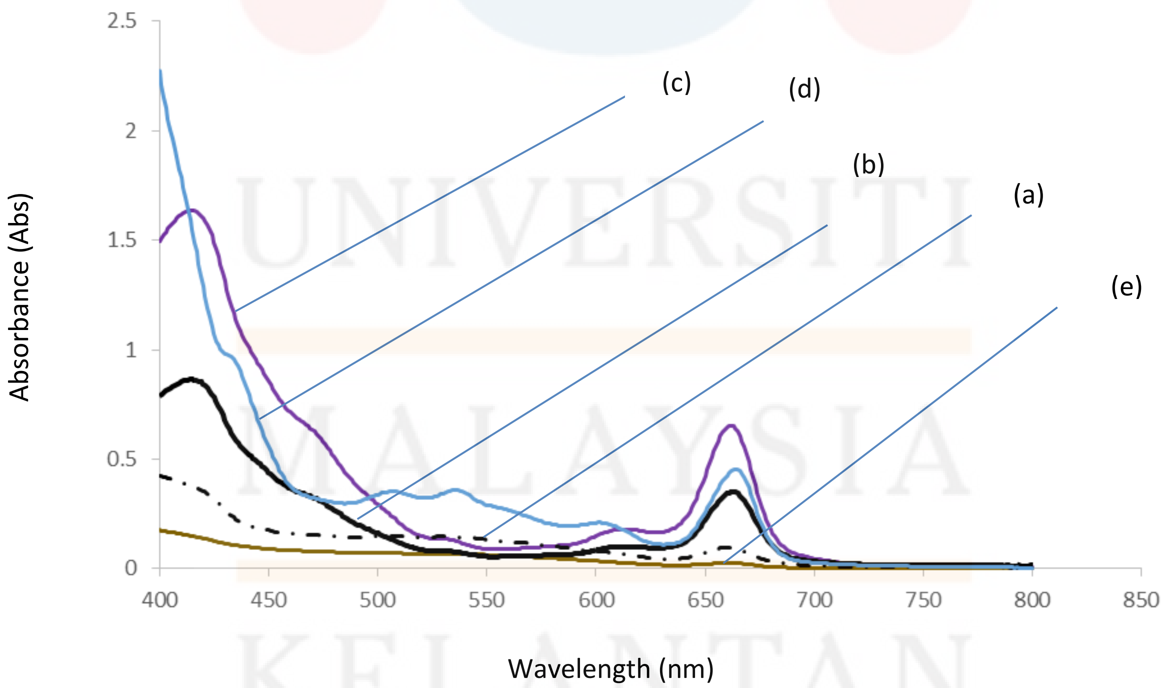

Figure 4.2 : UV absoption spectra of (a) **M**, (b) **S**, (c) 1 **M**: 10 **S**, (d) 3 **M**: 1 **S** and (e) 30 **M**: 1 **S** respectively

It can be seen from Figure 4.2 that *Sargassum binderi sp*. (seaweed, **S**) extract dye present strong absorption bands at wavelength of 470 nm and 680 nm. It is known that **S** has naturally occuring compound at wavelength of 420 nm and 720 nm, indicate the presence of flavonoids and chlorophyll (Davuluri *et al.*,2015). Chlorophyll is a green coloured pigment found is most of the plant which the function is to absorb sunlight and turn them into food. A green leaf absorbs blue light, mostly at 430 nm and red light, mostly at 660 nm. It reflects the green wavelengths, appearing green to human eye. Chlorophyll a, is found in blue-green algae and some red algae (İnanç, 2011). Chlorophyll exhibits an absorption band in the intense range of visible light due to charge-transfer transitions between the two highest occupied molecular orbitals (HOMO) and the two lowest unoccupied molecular orbitals (LUMO) in excited state. This is the reason why chlorophyll can be used as a good photo-absorber (Björn *et al.*, 2009).

While *Morus nigra L.* (mulberry, **M**) shows a present of distinct absorption band at 480 nm – 570 nm. Based on literature, the usual absorbance of wavelength for anthocyanin in **M** is from 450 nm – 575 nm (Hussain *et al.*, 2017). These broad UV absorption spectrum is related to the presence of triglycosides groups and the electron excitation from the $\pi \rightarrow \pi^*$ transition which is highly polar due to intramolecular charge transfer from the phenyl ring towards the carbonyl moiety (Zsila *et al*., 2003). The peak proved the presences of anthocyanins from mulberry fruits. Anthocyanins are generally accepted as the largest and most important group of water soluble pigments in nature (Harborne, 1998). The word anthocyanin derived from two Greek words anthos, which means flowers, and kyanos, which means dark blue (Horbowicz et al., 2008). Most of vegetables and fruits plant have the plentiful colour for attraction like red, blue, orange and yellow. This colour is directly proportional to the concentration of anthocyanins in the plant or fruit (Hussain et al,. 2017).

By combining **M** and **S** extract dye, it can be seen from the physical observation colour of the solution in the Figure 4.1 that the mixture were changed. UV-vis spectrum show both main peaks exist at the visible region. First, the mixture of 1**M**:10**S** shows the existence of peak around 630 nm – 680 nm and the main chlorophyll around 650 nm while peak for anthocyanin are not too visible as their amount are very tiny. The obvious absorption peak of chlorophyll and anthocyanin can be seen at 480 nm- 580 nm and 630 nm – 680 nm with increasing ratio of mulberry 3 **M** : 1 **S**. This might be due to the change of structural properties occur due the mixing of dye extract. As shown, by mixing the extract dye with ratio 3 **M**:1 **S**, both of distinct peak for both individual dyes (**M** and **S**) were observed.. Next, for ratio 30 **M**:1 **S** , it can be seen from the figure that peak of chlorophyll does not clearly visible as the ratio is very low compared to ratio of anthocyanin.

Overall, the presence of main peaks derived from both original dyes extracts could be observed. It is believed that the changes of photo-absorption properties were occurred. However, further analysis should be carried out in order to understand deeper about the characteristic of this newly found mixed extracts dyes.

4.4 Thermogravimetric Analyzer (TGA)

Thermogravimetric analysis is an analysis in which the mass of sample is measured over time as the temperature changes. This analysis also figured out the melting point state of sample degradation and percentage of weight loss. The samples of *Morus nigra L.* (mulberry) (**M**) showed rapid weight loss at around 140 °C resulting from the evaporation of residual solvent and another weight loss at around 360 °C corresponding to the decomposition of organic compounds (Banerjee *et al,*, 1993). While the sample of *Sargassum binderi sp.* (seaweed) (**S**) showed rapid weight loss around 200 °C resulting from the evaporation of excessive solvent inside the sample itself and another weight loss around 750 °C due to the sample is decomposed. By this analysis it can be concluded that **S** has higher melting point than **M.** Figure 4.3 and figure 4.4 below show the thermogravimetric analysis of both single dye samples.

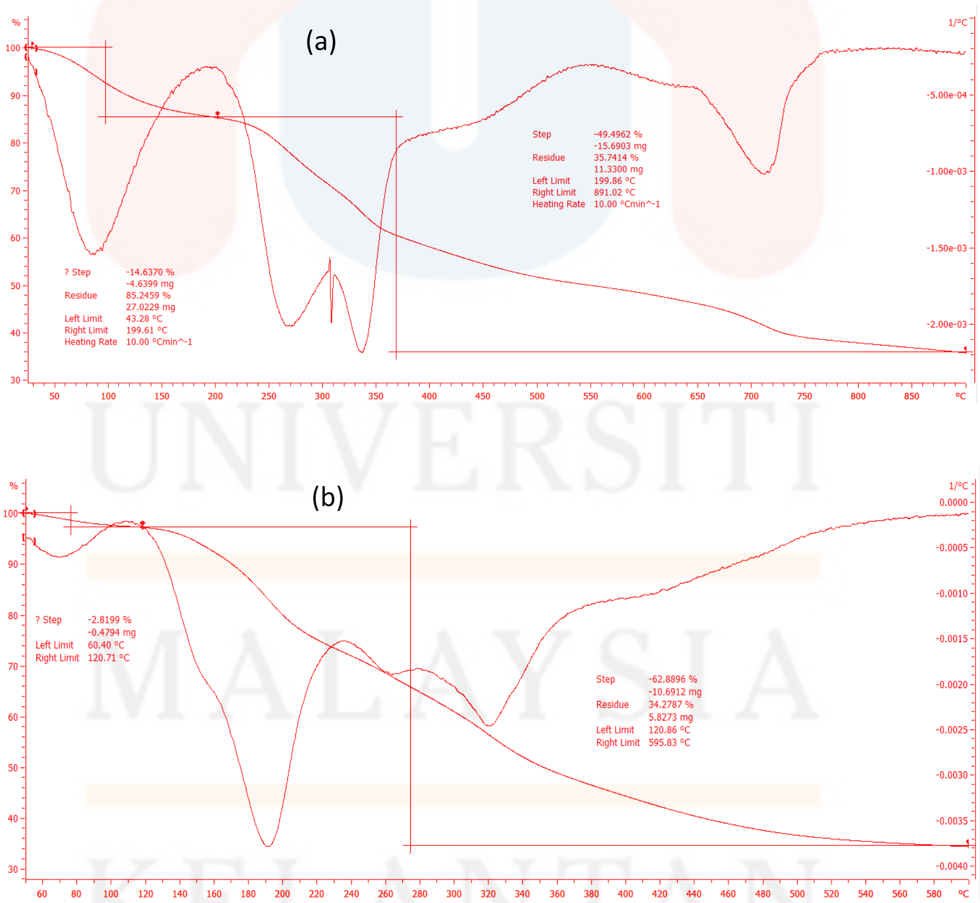

Figure 4.3: (a) TGA analysis of *Sargassum binderi sp.* (seaweed, **S**); (b) TGA analysis for *Morus nigra L.* (mulberry, **M**)

4.5 Scanning Electron Microscope (SEM)

SEM image is an image that obtained by scanning the surface with an electron beam and capturing either the electrons refracted or electrons emitted from various locations of the material. The sample has to be a good conductor to accept the electron flow. In this study, the surface morphology of the dyes nanoparticles was viewed using Scanning Electron Microscope (SEM) HACH DR6000.

As shown in Figure 4.5 (a), it can be seen that the **M** dye particles on titanium dioxide (TiO_2) were in porous structure with smooth surface. Meanwhile, the analysis result of SEM for **S** on TiO_2 as shown in the Figure 4.5 (b), revealed dye particle on granul size on the TiO_2 pores.

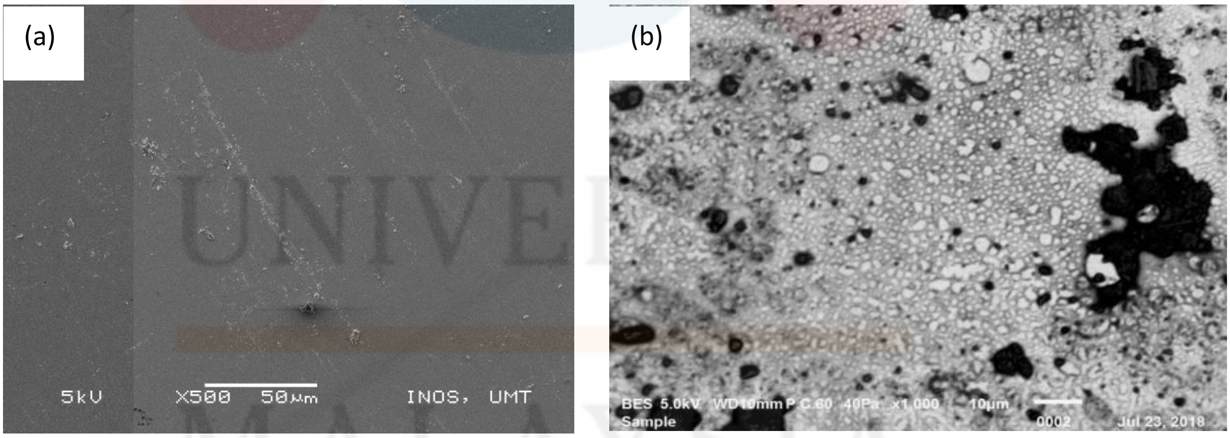

Figure 4.4: (a) SEM image from *Morus nigra L.* (mulberry, **M**) and (b) *Sargassum binderi sp.* (seaweed, **S**), respectively.

From the Figure 4.6 it can be seen that the existance of both distinct shapes of both individual dye (**M** and **S**). Hence, it can be concluded that the mixing of both dye were successfully done.

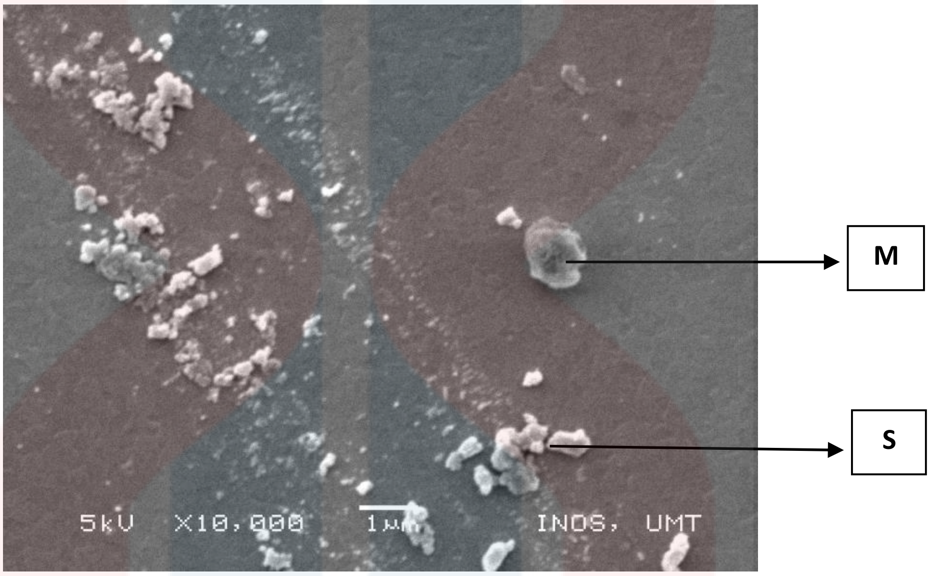

Figure 4.5: SEM image of the mixed dye 30**M**: 1**S** on ITO glass.

4.6 The Conductivity Measurement

In this study, four point probe were used to measure the flow of voltage of the conductive samples. Four point probe had been used to test the conductivity of the surface layer of dye-sensitized solar cell (DSSC). Table 4.1 summarize the result of the conductivity layer where the analysis were conducted in two different situations which are under dark condition and with light presence. The comparison was done in between both individual dye samples and the mixed ratio dye samples (1**M**:10**S**, 3**M**:1**S**, and 30**M** : 1**S**) that had been prepared.

Table 4.1: The conductivity values of the surface of the dye extracts.

	Dark (0 W/M^2)		Light (200W/M^2)	
	σ = 1/Rs (Ω^{-1} m^{-1})	σ = 1/Rs (Scm^{-1})	σ = 1/Rs (Ω^{-1} m^{-1})	σ = 1/Rs (Scm^{-1})
M	1.19E-02	1.19E-04	2.34E-02	2.34E-04
S	2.17E-02	2.17E-04	4.36E-02	4.36E-04
1**M**:10**S**	1.94E-02	1.94E-04	3.89E-02	3.89E-04
3 **M**:1**S**	2.20E-02	2.20E-04	4.39E-02	4.39E-04
30**M**:1**S**	2.01E-02	2.01E-04	3.34E-02	3.34E-04

Based on the table 4.1, the highest conductivity measurement was recorded from 3**M**:1**S** for dark condition with 0.0220 Ω^{-1} m^{-1} while for light condition is 0.0439 Ω^{-1} m^{-1}. By comparing with only individual dye **M** performed 0.0119 Ω^{-1} m^{-1} while **S** conducted 0.0234 Ω^{-1} m^{-1}. It can be concluded that the mixed dye has higher conductivity than single dye. Thus, study confirmed with the analysis of these dyes in dye-sensitized solar cell (DSSC).

Since four point probes only measure the surface conductivity of the extract dye, digital multimeter was used to measure the conductivity of the whole device. There are 3 parameters were set for right distance which are 5 cm, 10 cm and 15 cm.

From the obtained result, as listed in Table 4.2, mixed dye sample recorded higher conductivity value compared to individual extract dyes (**M** and **S**). In this analysis, the highest conductivity was recorded by 30**M**:1**S** with the value 0.629 V followed by the 3**M**:1**S** with the value of 0.563 at the distance of 15 cm from source of light . The result pattern was found similar trend to the previous analysis by four point probe, which mixed dyes can conduct more electricity compare to single dye.

Table 4.2 **:** The conductivity value of the whole dyes - sensitized solar cell devices.

Distance (cm)	**M** (V)	**S** (V)	1**M**:10**S** (V)	3**M**:1**S** (V)	30**M**:1**S** (V)
5 cm	0.106	0.094	0.078	0.432	0.593
10 cm	0.098	0.080	0.046	0.572	0.595
15 cm	0.154	0.078	0.057	0.563	0.629

4.7 Current Voltage (IV) Measurement

The application of **M, S** and mixed dye (1 **M**: 10 **S**, 3 **M**: 1 **S** and 30 **M**: 1 **S**) in solar cell device was evaluated after device fabrication of ITO/TiO_2/dye **M, S,**1 **M**: 10 **S**, 3 **M**: 1 **S** and 30 **M**: 1 **S**)/ carbon/aluminium. The current voltage measurement was carried out using Electrochemical Impendence Spectroscopy (EIS) (Metrohm Autolab) to measure the solar cell performance of dye-sensitized solar cell (DSSC). In this analysis, the maximum photocurrent (Imax), the maximum photovoltage (Vmax), the short circuit photocurrent (Isc), and the open circuit photovoltage (Vsc) can be obtained from IV curve shown on the appendix. Maximum power (Pmax) of DSSC was calculated from the formula : Pmax =(I x V). I is the current value in ampere (A) and V is the voltage in (Mv). FF value was obtainesd using the formula FF = (I x V) max/ (Isc x Voc).

Table 4.3: Solar cell parameter obtained of all fabricated devices.

	Vmax	Imax	Voc	Isc	Pin	Pmax	PCE	FF
M	1.51E-01	1.25E-07	2.93E-01	2.43E-07	2.00E-05	1.88E-08	9.20E-02	2.64E-02
S	2.00E-01	3.70E-07	4.73E-01	7.80E-07		7.37E-08	3.68E-02	2.01E-02
1**M**:10**S**	1.76E-01	4.09E-07	3.63E-01	8.20E-07		7.26E-08	3.63E-02	2.42E-02
3**M**:1**S**	2.80E-01	2.45E-07	6.15E-01	1.32E-02		6.93E-08	3.47E-02	1.57E-02
30**M**:1**S**	2.03E-01	1.26E-06	4.37E-01	2.62E-06		1.89E-07	9.44E-02	1.57E-02

From the results, it show that mixed dye performed higher solar efficiency compared to the individual dye (**M** and **S**), as example, the mixed ratio of 30 **M**:1 **S** formed 9.44×10^{-02} % of solar efficiency with **M** and **S** only 9.2×10^{-02} % and 3.68×10^{-02} % respectively. This may occur because the high sensitization process after mixing process of the two single dye and the change in its composition. Whilst the lowest solar cell efficiency recorded from the mixture of 3**M**:1**S** with the value of 3.47×10^{-02} %. This may happen due to the mixture might be not fully optimized during the process of mixing. Further study should be carried out to find out the best ratio of these mixed dye.

CHAPTER 5

CONCLUSION AND RECOMMENDATION

5.1 Conclusion

The extracts dyes of *Morus Nigra L*. (mulberry, **M**) and *Sargassum Binderi Sp.* (seaweed, **S**) and the hybrid dyes of 1**M** : 10**S**, 3**M** : 1**S**, and 30**M** : 1**S** were successfully extracted and prepared. The characterisation of the extract dyes were observed by Ultraviolet-visible spectroscopy (UV-Vis), bandgap evaluation, conductivity, Scanning Electron Microscopy (SEM), thermogravimetric analysis (TGA) and differential scanning calorimetry (DSC) and 4 point probe.

From the UV-vis analysis that was conducted, the absorption spectra of *Morus Nigra L*. (mulberry, **M**) and *Sargassum Binderi Sp.* (seaweed, **S**) dye solutions were observed at the different wavelength region based on the sample. *Sargassum Binderi sp*. (**S**) extract dye can be found strong absorption bands at wavelength of 420 nm and 720 nm to represent of anthocyanin and chlorophyll. The main peak of both *Morus Nigra L*. (mulberry, **M**) and *Sargassum Binderi Sp.* (seaweed, **S**) were also detected in the absorption spectra of hybrid solutions. The mixing ratio of each extracts dyes also influenced the intensity and shift of absorption spectra, probably due to the changes of the photo-absorption properties.

The thermogravimetric analysis is where to measure the loss of mass of sample over time as the temperature changes. The *Sargassum binderi sp*. (seaweed, **S**) showed the higher melting point than *Morus nigra L.* (mulberry, **M**). **M** showed rapid weight loss at around 140 °C and at around 360 °C due to the decomposition of organic compounds. The sample of **S** showed rapid weight loss around 200 °C because of the excessive solvent and another 750 °C due to decomposition.

Besides that, scanning electron microscopy (SEM) is used to observe the surface morphology of dye nanoparticles. **M** morphology represented big shaped particles existed on TiO_2 surface while SEM images of the mixed dye showed the existence of distinct structure from individual dye.

The four point probe showed the highest result in conductivity measurement from 3 **M**:1 **S**. Among other samples as compared with individual dye (**M** and **S**) for both light and dark condition with 2.20E-02 Ω^{-1} m^{-1} and is 4.39E-02 Ω^{-1} m^{-1} while the lowest result is single dye which is mulberry. The value for both dark and light condition is 1.19E-02 **Ω**-1 m-1 and 2.34E-02 Ω^{-1} m^{-1}. The current voltage measurement was studied to measure the solar cell performance of dye-sensitized solar cell (DSSC). The result showed that mixed ratio of 30 **M**:**1** S where the value is 9.44E-02 % which is the highest value among others and the lowest is solar cell efficiency is the mixture of 3**M**:1**S** with the value of 3.47E-02 %.

5.2 Recommendation

In this study, the important lf quality of dyes pigment which may lead to obtain high solar efficiency. In future there should be more study on this matter by trying new type of natural extract dyes. The approach in preparing hybrid dyes solution with other natural dyes also should be studied in future.

However, the extraction of natural dye needs to be optimized to get the highest yield and best quality of dye pigment. To avoid any, the extraction and device fabrication need to be handled in a right way. The sample of solution that was extracted should be properly stored under dark condition and at suitable temperature to avoid any bacterial growth and inconsistency data. Besides to avoid from any degradation of dye, the preparation sample must be done under non-direct sunlight.

Meanwhile, other precaution steps should be carried out to avoid errors during measurement. Lastly, to tune the photo-absorber properties of extract dye, other parameters can be studied in the future such as the pH control, temperature and different solvent used in the extraction.

REFERENCES

A, A. R., & Davuluri, D. (2015). Extraction of dye from marine macroalgae, *International Journal of ChemTech Research*, 8(3), 1060-1063

Abbasian, K., Rostami, a., & Pourkhorshidi, S. (2012). Design of hybrid solar cell based on dye-sensitized TiO_2 nanoparticles with conjugated polymer. *Acta Physica Polonica A*, *121*(1), 10–12.

Al-Bat'hi, S. a M., Alaei, I., & Sopyan, I. (2013). Natural photosensitizers for dye sensitized solar cells. *International Journal of Renewable Energy Research*, *3*(1), 138–143.

Aramwit, P., Bang, N., & Srichana, T. (2010). The properties and stability of anthocyanins in mulberry fruits. *Food Research International*, *43*(4), 1093–1097.

Ayalew W. A. and Ayele D. W. (2016). Dye-Sensitized Solar Cells Using Natural Dye As Light-Harvesting Materials Extracted From Acanthus Sennii Chiovenda Flower And Euphorbia Cotinifolia Leaf. *Journal of Science: Advanced Materials and Devices, Volume 1, Issue 4,* 488-494.

Baxter, R., Hastings, N., Law, a., & Glass, E. J. . (2008). A rapid and robust sequence-based genotyping method for BoLA-DRB3 alleles in large numbers of heterozygous cattle. *Animal Genetics*, *39*(5), 561–563.

Bhatia S. C. (2014). Energy Resources and Their Utilisation. *Journal Advanced Renewable Energy Systems*, 1-31.

Bertolli, M. (2008). Solar Cell Materials. *Solar Cell Materials: Developing Technologies*, 1-13

Björn, L. O., Papageorgiou, G. C., Blankenship, R. E., & Govindjee. (2009). A viewpoint: Why chlorophyll a, *Photosynthesis Research*, *99*(2), 85–98.

Čekon, M., & Rovnaník, P. (2015). Optical Performance of Colored Crystalline Solar Cells for Building Energy Efficient Application. *Procedia Manufacturing*, 342–347.

Cerda, B., Sivakumar, R., & Paulraj, M. (2016). Natural dyes as sensitizers to increase the efficiency in sensitized solar cells. *Journal of Physics: Conference Series*, Vol *720*(1).

Chopra, K. L., Paulson, P. D., & Dutta, V. (2004). Thin-film solar cells: an overview. *Progress in Photovoltaics: Research and Applications*, *12*(23), 69–92.

Collins, P. G., Bradley, K., Ishigami, M., & Zettl, A. (2000). Extreme oxygen sensitivity of electronic properties of carbon nanotubes. *Science (New York, N.Y.)*, *287*(5459), 1801–1804.

Ginger, D. S., & Greenham, N. C. (1999). Photoinduced electron transfer from conjugated polymers to CdSe nanocrystals. *Physical Review B*, *59*(16), 10622–10629.

Gong J., K. Sumathy., Qiquan Qiao, Z. Z. (2017). Review On Dye-Sensitized Solar Cells (Dsscs): Advanced Techniques And Research Trends. *Journal Renewable and Sustainable Energy Reviews*, 234-246.

Guarracino, P., Gatti, T., Canever, N., Abdu-Aguye, M., Loi, M. A., Menna, E., & Franco, L. (2017). Probing photoinduced electron-transfer in graphene–dye hybrid materials for DSSC. *Phys. Chem. Chem. Phys.*, *19*(40), 27716–27724.

Horbowicz, Marcin & Kosson, R & Grzesiuk, A & Dębski, Henryk. (2008). Anthocyanins of fruits and vegetables-their occurrence, analysis and role in human nutrition. *Vegetable Crops Research Bulletin*, Vol 68, 5-22.

Hussain, F., Rana, Z., Shafique, H., Malik, A., & Hussain, Z. (2017).

Phytopharmacological potential of different species of Morus alba and their bioactive phytochemicals: A review. *Asian Pacific Journal of Tropical Biomedicine*, *7*(10), 950–956.

İnanç, A. L. (2011). Chlorophyll: Structural Properties, Health Benefits and Its Occurrence in Virgin Olive Oils. *Akademik Gıdatr (A.L. İnanç)*, *9*(2), 90–344.

Jager, K., Isabella, O., Smets, A. H. M., Swaaij, R. A. C. M. M. van, & Zeman, M. (2014). Solar Energy Fundamentals, Technology and Systems. *Delf University of Technology*, 1–420.

Jingcheng, L. (2010). Application of solar energy. *Solar Energy*, *3*(3), 48.

Jones, G., & Bouamane, L. (2012). Power from Sunshine: A Business History of Solar Energy. *Harvard Business School*, 12-105.

Kao Circle, Manassas C, U. S. E. (2017). Energy Consumption (pp. 45–49).

László, D. K. (2015). Anthocyanins, *Semmelweis University Department of Pharmacognosy*, 1–37.

O'Regan, B., & Grätzel, M. (1991). A low-cost, high-efficiency solar cell based on dye-sensitized colloidal TiO2 films. *Nature*, *353*(6346), 737–740.

Osabohien, E. (2014). Extraction and application of dyestuffs from the leaves of guinea corn and onion skin. *International Journal of Biological and Chemical Sciences*, *8*(April), 811–820.

Rehm, J. M., McLendon, G. L., Nagasawa, Y., Yoshihara, K., Moser, J., & Grätzel, M. (1996). Femtosecond Electron-Transfer Dynamics at a Sensitizing Dye−Semiconductor (TiO_2) Interface. *The Journal of Physical Chemistry*, *100*(23), 9577–9578.

Rhanabat K., A. A. Revina, L. Patrikev, K. A. (2016). An Introduction To Solar Cell Technology. *Ipp Review Paper*, 481-491.

Saxena, S., & Raja, A. S. M. (2015). Roadmap to Sustainable Textiles and Clothing. *Central Institute for Research on Cotton Technology*, 37-80.

Sharma, S., Jain, K. K., & Sharma, A. (2015). Solar Cells: In Research and Applications—A Review. *Materials Sciences and Applications*, *6*(12), 1145–1155. Shawley N. and Soumitra Satapathi. (2017). Utilization of Naturally Occurring Dyes as Sensitizers in Dye Sensitized Solar Cells. *Ieee Journal Of Photovoltaics*, Vol. 7, 539-544.

Sumardiasih, S., Obina, W. M., A Talip, L. F., Ramli, M. M., M Isa, S. S., C Halin, D. S., Muda, M. R. (2017). Hybrid TiO_2 Gigantochloa Albociliata Charcoal in Dye Sensitized Solar Cell Characteristics of dye Rhoeo spathacea in dye sensitizer solar cell (DSSC). *Series: Materials Science and Engineering*, *209*.

Swami, R. (2012). Solar Cell. *International Journal of Scientific and Research Publications*, *2*(7), 1–5.

Wahyuono, R. A., & Risanti, D. D. (2012). Selection of Natural Dye Photosensitizer for Quasi-solid State Dyesensitized Mesoporous TiO_2 Solar Cell (DSC) Fabrication. *Proceeding International Conference of Chemical and Material Engineering*, (September), 1–6.

World Energy Council. (2013). World Energy Resources: 2013 survey. *World Energy Council*, 11.

Yang, J., Bark, C., Kim, K., & Choi, H. (2014). Characteristics of the Dye-Sensitized Solar Cells Using TiO_2 Nanotubes Treated with TiCl4. *Materials*, *7*(5), 3522–3532.

Yip, W. H., Lim, S. J., Mustapha, W. A. W., Maskat, M. Y., & Said, M. (2014). Characterisation and stability of pigments extracted from Sargassum binderi obtained from Semporna, Sabah. *Sains Malaysiana*, *43*(9), 1345–1354.

Yuri Tsuruda, A., Lima De, M., Filho, M., Busanello, M., Guergoletto, K., Tahis, R., Garcia, S. (2013). Differentiated Foods for Consumers with New Demands. *ResearchGate Journal*, 163-190.

Zsila, F., Bikádi, Z., Simonyi, M. (2003). Probing the binding of the flavonoid, quercetin to human serum albumin by circular dichroism, electronic absorption 300 spectroscopy and molecular modelling methods, *Biochem Pharmacol.*, 447-56.

APPENDIX A

(RESULT AND DATA ANALYSIS)

Data A.1 : IV curve for 1**M :** 10**S**

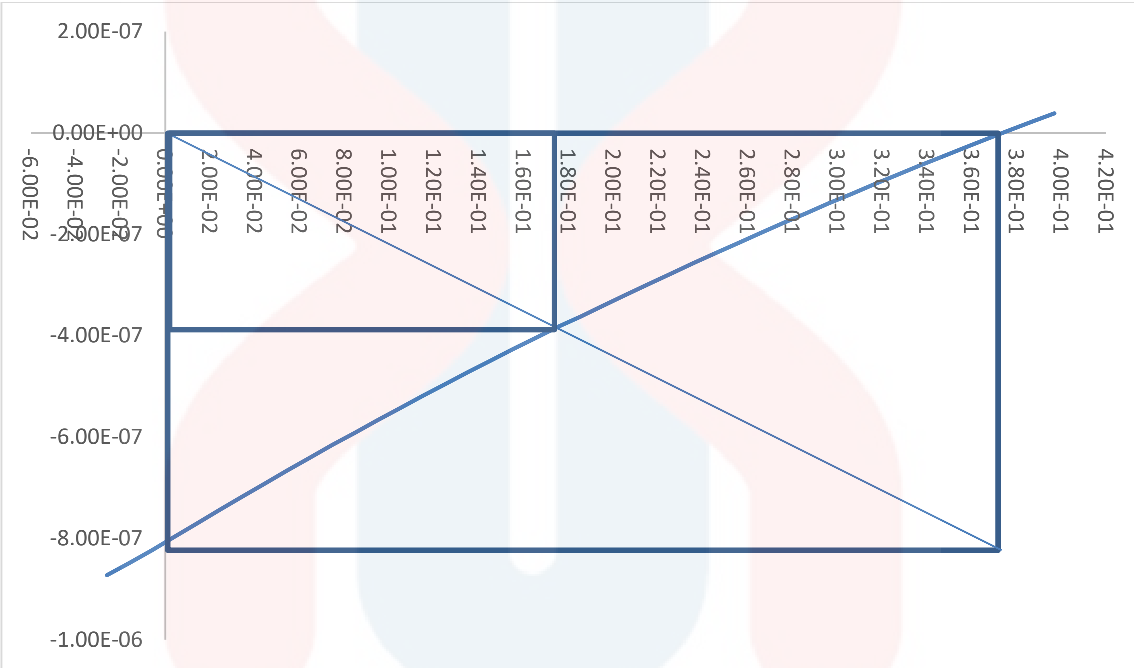

Vmax	1.75E-01	
Imax	3.97E-07	
Voc	3.67E-01	
Isc	7.97E-07	
Pin	2.00E-04	
Pmax	6.95E-08	Vmax*Imax
EFF	0.034738	(Pmax/Pin)*100
FF	2.38E-01	(Imax*Vmax)\Isc*Voc)

Data A.2 : IV curve for 3M : 1S

Vmax	2.85E-01	
Imax	2.00E-07	
Voc	6.18E-01	
Isc	4.68E-07	
Pin	2.00E-04	
Pmax	5.70E-08	Vmax*Imax
EFF	0.0285	(Pmax/Pin)*100
FF	1.97E-01	(Imax*Vmax)\Isc*Voc)

Data A.3 : IV curve for 30M : 1S

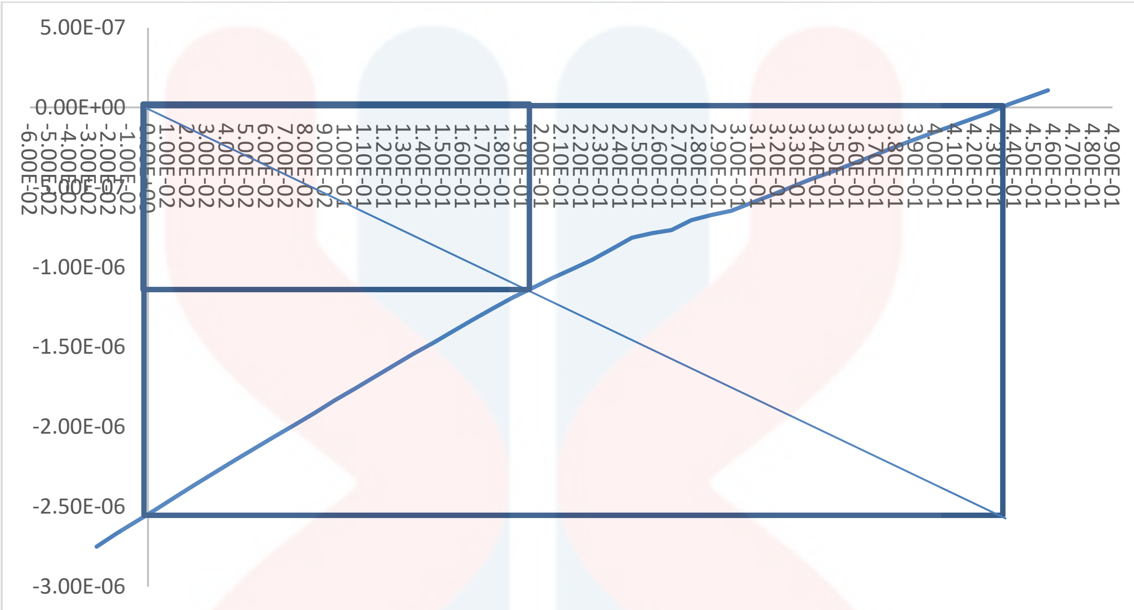

Vmax	1.95E-01	
Imax	1.20E-07	
Voc	4.27E-01	
Isc	2.52E-06	
Pin	2.00E-04	
Pmax	2.34E-08	Vmax*Imax
EFF	1.17E-02	(Pmax/Pin)*100
FF	2.17E-02	(Imax*Vmax)\Isc*Voc)

Data A.4 : IV curve for **M**

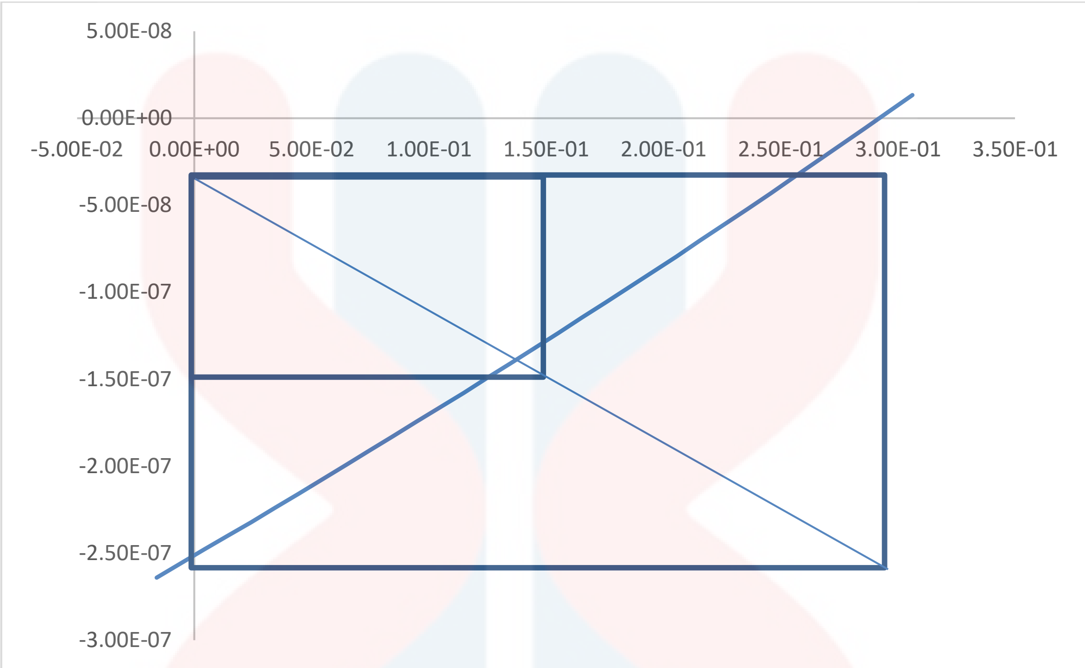

Vmax	1.55E-01	
Imax	1.23E-07	
Voc	2.86E-01	
Isc	2.48E-07	
Pin	2.00E-04	
Pmax	1.91E-08	Vmax*Imax
EFF	0.009533	(Pmax/Pin)*100
FF	2.69E-01	(Imax*Vmax)\Isc*Voc)

Data A.5: IV curve for **S**

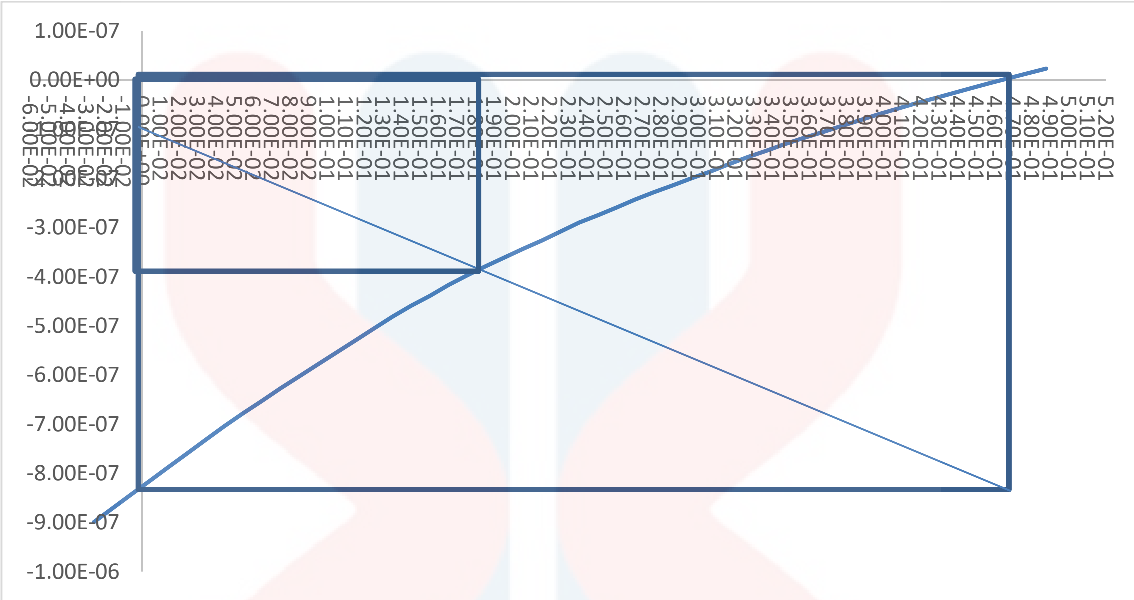

Vmax	1.82E-01	
Imax	3.80E-07	
Voc	4.57E-01	
Isc	8.15E-07	
Pin	2.00E-04	
Pmax	6.92E-08	Vmax*Imax
EFF	0.03458	(Pmax/Pin)*100
FF	1.86E-01	(Imax*Vmax)\Isc*Voc)